Chapter 3

Effects of Mass Factor on Halo orbits about collinear Lagrangian points in CRTBP

3.1 Introduction

In the previous chapter, an initial guess of halo orbits around collinear Lagrangian points is obtained upto the fifth order approximation using Lindstedt-Poincaré method, and the effects of perturbations due to radiation pressure and oblateness of the primaries on parameters of halo orbits are analyzed. By considering various perturbations, different researchers have found halo orbits in several systems. The Sun-Earth system has been considered by Srivastava et al. (2016), Tiwary and Kushvah (2015), the Sun-Earth+Moon system by Pal and Kushvah (2015), the Sun-Mars system by Eapen and Sharma (2014), the Saturn-Satellite system by Pushparaj and Sharma (2016), the Antares-Sun-Proxima Centauri system by Ghotekar and Sharma (2019), and Mishra and Jha (2020) have considered the Sun-Venus system. The locations and parameters of halo orbits vary in each Sun-Planet system. Also, from equations (1.30), (1.32) and (1.34), it can be observed that the roots of these polynomials depend on the values of A_1, A_2, q_1, q_2 and μ. So, locations of Lagrangian points depend on the value of mass factor of primaries as well. Further, expressions (2.14) and (2.15) for C_m also depend on μ, hence parameters of halo orbits around all three collinear Lagrangian points also depend on the value of μ. So, it is pertinent to examine the effects of mass factor μ on different parameters of the system.

In this chapter, by using the fifth order approximate solution, variations in the parameters of halo orbits around collinear Lagrangian points due to variations in the

value of mass factor μ of primaries are studied. For inspecting the changes in parameters of halo orbits, different values of μ in the interval $[10^{-8}, 0.5]$ are considered. For validating the results, five different Sun-Planet systems are considered.

3.2 Computation of Orbital Parameters

For analyzing the variations in locations of collinear Lagrangian points, equations (1.30), (1.32) and (1.34) are solved by neglecting the perturbations due to radiation and oblateness of the primaries. So, $A_1 = A_2 = 0$ and $q_1 = q_2 = 1$. Then equations (1.30), (1.32) and (1.34) reduce to

$$\gamma^5 - (3-\mu)\gamma^4 + (3-2\mu)\gamma^3 - \mu\gamma^2 + 2\mu\gamma - \mu = 0, \tag{3.1}$$

$$\gamma^5 + (3-\mu)\gamma^4 + (3-2\mu)\gamma^3 + \mu\gamma^2 + 2\mu\gamma + \mu = 0, \tag{3.2}$$

$$\gamma^5 + (2+\mu)\gamma^4 + (1+2\mu)\gamma^3 + (1-\mu)\gamma^2 + 2(1-\mu)\gamma + (1-\mu) = 0, \tag{3.3}$$

respectively. Equations (3.1)-(3.3) are solved for γ by considering different values of μ, using which the locations of Lagrangian points can be obtained.

The period, T, of halo orbits can be obtained from

$$T = \frac{2\pi}{\lambda\omega},$$

where ω and λ are as given in Chapter 2.

For analyzing the variation in x-amplitude, $A_{\tilde{x}}$, its value is obtained using the amplitude constraint

$$l_1 A_{\tilde{x}}^2 + l_2 A_{\tilde{z}}^2 + \Delta = 0$$

by selecting a particular value of z-amplitude, $A_{\tilde{z}}$. In above amplitude constraint relation, the quantities l_1 and l_2 are as described by Richardson (1980).

The state vector of a spacecraft moving in a halo orbit at any time can be obtained using the equations (2.26). Substituting $\tau = 0$ in equations (2.26), the components of

position vector at initial time are obtained as

$$\begin{aligned}
\widetilde{x}(0) &= (\rho_{20}+\rho_{40}) - A_{\tilde{x}}\cos\phi + (\rho_{21}-\rho_{22}+\rho_{41})\cos 2\phi \\
&\quad + (\rho_{31}+\rho_{51})\cos 3\phi + \rho_{42}\cos 4\phi + \rho_{52}\cos 5\phi, \\
\widetilde{y}(0) &= (kA_{\tilde{x}}+\sigma_{32}+\sigma_{51})\sin\phi + (\sigma_{21}+\sigma_{41}-\sigma_{22})\sin 2\phi \\
&\quad + (\sigma_{31}+\sigma_{52})\sin 3\phi + \sigma_{42}\sin 4\phi + \sigma_{53}\sin 5\phi, \\
\widetilde{z}(0) &= (-1)^{\frac{p-1}{2}}(A_{\tilde{z}}\cos\phi + k_{21}\cos 2\phi + k_{22} + k_{32}\cos 3\phi) \\
&\quad + k_{40} + k_{41}\cos 2\phi + k_{42}\cos 4\phi + k_{51}\cos 3\phi + k_{52}\cos 5\phi,
\end{aligned} \tag{3.4}$$

and the components of velocity vector at initial time are

$$\begin{aligned}
\widetilde{x}'(0) &= \lambda A_{\tilde{x}}\sin\phi - 2\lambda(\rho_{21}-\rho_{22}+\rho_{41})\sin 2\phi \\
&\quad - 3\lambda(\rho_{31}+\rho_{51})\sin 3\phi - 4\lambda\rho_{42}\sin 4\phi - 5\lambda\rho_{52}\sin 5\phi, \\
\widetilde{y}'(0) &= \lambda(kA_{\tilde{x}}+\sigma_{32}+\sigma_{51})\cos\phi + 2\lambda(\sigma_{21}+\sigma_{41}-\sigma_{22})\cos 2\phi \\
&\quad + 3\lambda(\sigma_{31}+\sigma_{52})\cos 3\phi + 4\lambda\sigma_{42}\cos 4\phi + 5\lambda\sigma_{53}\cos 5\phi, \\
\widetilde{z}'(0) &= (-1)^{\frac{p+1}{2}}\lambda(A_{\tilde{z}}\sin\phi + 2k_{21}\sin 2\phi + 3k_{22} + k_{32}\sin 3\phi) \\
&\quad - 2\lambda k_{41}\sin 2\phi - 4\lambda k_{42}\sin 4\phi - 3\lambda k_{51}\sin 3\phi - 5\lambda k_{52}\sin 5\phi,
\end{aligned} \tag{3.5}$$

where $p = 1, 3$. Since the origin is shifted to the Lagrangian point for obtaining halo orbits, the elements of the initial state vector in a coordinate system with the origin at the barycentre of the primaries can be obtained using the relations

$$x(0) = L_i + \gamma\widetilde{x}(0), \quad y(0) = \gamma\widetilde{y}(0), \quad z(0) = \gamma\widetilde{z},$$

where $i = 1, 2, 3$ and

$$x'(0) = \gamma\widetilde{x}'(0), \quad y'(0) = \gamma\widetilde{y}'(0), \quad z'(0) = \gamma\widetilde{z}'(0).$$

3.3 Results and Discussion

Here, changes in location of Lagrangian points and changes in amplitude, period, size, initial position and initial velocity of halo orbits are examined. Locations of collinear Lagrangian points, halo orbits and parameters of these orbits are computed in a dimensionless system. The Sun-Mars, Sun-Earth, Sun-Uranus, Sun-Saturn and Sun-Jupiter systems are considered for validating the results.

3.3.1 Variations in location of Lagrangian points

In Fig. 3.1, variation in location of Lagrangian points L_1 and L_2 due to variation in the value of μ, the mass factor of the primaries, is shown. The minimum value of mass factor is $\mu = 10^{-8}$ which is increased by a fixed step size of 10^{-6} until μ becomes 0.5.

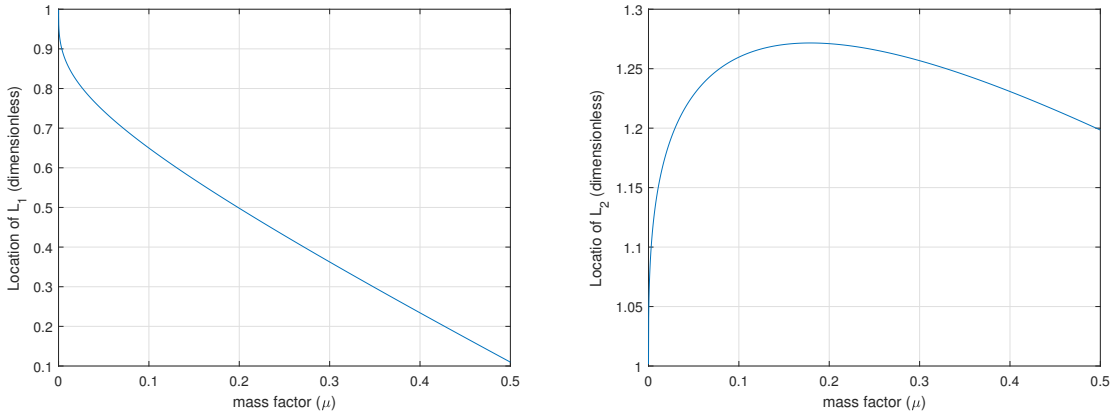

(A) Variation in location of L_1 (B) Variation in location of L_2

FIGURE 3.1: Variation in location of Lagrangian points against variation in mass factor

From Fig. 3.1(A), it can be concluded that with the increase in the value of mass factor of the primaries, Lagrangian point L_1 recedes from the second primary and shifts towards the more massive primary. The variation in location of L_2 is given Fig. 3.1(B). The location of L_2 is a non-monotonic function of μ. With the increase in the value of μ, L_2 moves away from the second primary, in the opposite direction of the first primary P_1, until $\mu_0 \approx 0.17894$ and for $\mu \geqslant \mu_0$, L_2 comes closer to P_2, the second primary.

In Tables 3.1 and 3.2, parameters of halo orbits around L_1 and L_2, respectively, are given for different Sun-Planet systems. Since collinear Lagrangian points lie on the line joining the primaries, y and z coordinates of L_1 and L_2 are zero. So, only x coordinate of L_1 and L_2 is given Tables 3.1 and 3.2. From Table 3.1, it can be observed that as the value of mass factor increases, the value of x coordinate of L_1 decreases which shows the Lagrangian point L_1 goes nearer to the Sun. In Table 3.2, the value of x coordinate of L_2 increases as the value of μ increases which means L_2 recedes from the second primary. Here, the highest value of mass factor corresponds to the Sun-Jupiter system with $\mu = 9.5367 \times 10^{-4} \leqslant \mu_0$, so L_2 goes away from the second primary in all cases.

In Table 3.3, location of L_3, z-amplitude, $A_{\tilde{z}}$ and period of halo orbits in the Sun-Mars, Sun-Earth, Sun-Earth+Moon, Sun-Saturn and Sun-Jupiter system are given. As the

TABLE 3.1: Dimensionless parameters of halo orbits around L_1 for different Sun-Planet systems

System	mass factor (μ)	L_1	$A_{\tilde{x}}$	Period	initial distance	initial velocity
Sun - Mars	3.2271×10^{-7}	0.99526	0.13580	3.05791	0.99599	0.00451
Sun - Earth	3.0035×10^{-6}	0.99009	0.13379	3.03520	0.99160	0.00943
Sun - Earth+Moon	3.0404×10^{-6}	0.99005	0.13378	3.03503	0.99157	0.00947
Sun - Uranus	4.3656×10^{-5}	0.97612	0.12847	2.97449	0.97962	0.02261
Sun - Saturn	2.8573×10^{-4}	0.95602	0.12109	2.88917	0.96209	0.04121
Sun - Jupiter	9.5367×10^{-4}	0.93509	0.11385	2.80375	0.94347	0.05992

TABLE 3.2: Dimensionless parameters of halo orbits around L_2 for different Sun-Planet systems

System	mass factor (μ)	L_2	$A_{\tilde{x}}$	Period	initial distance	initial velocity
Sun - Mars	3.2271×10^{-7}	1.00476	0.13878	3.08879	1.00531	0.00418
Sun - Earth	3.0035×10^{-6}	1.01003	0.14002	3.09983	1.01120	0.00882
Sun - Earth+Moon	3.0404×10^{-6}	1.01008	0.14003	3.09991	1.01125	0.00886
Sun - Uranus	4.3656×10^{-5}	1.02457	0.14345	3.12998	1.02750	0.02172
Sun - Saturn	2.8573×10^{-4}	1.04607	0.14855	3.17415	1.05178	0.04114
Sun - Jupiter	9.5367×10^{-4}	1.06883	0.15403	3.22086	1.07772	0.06226

TABLE 3.3: Dimensionless parameters of halo orbits around L_3 for different Sun-Planet systems

System	mass factor (μ)	L_3	$A_{\tilde{z}}$	Period
Sun - Mars	3.2271×10^{-7}	-1.000000	0.1550735	6.28318
Sun - Earth	3.0035×10^{-6}	-1.000001	0.1550987	6.28317
Sun - Earth+Moon	3.0404×10^{-6}	-1.000001	0.1550990	6.28316
Sun - Saturn	2.8573×10^{-4}	-1.000119	0.1577230	6.28161
Sun - Jupiter	9.5367×10^{-4}	-1.000397	0.1637293	6.27796

value of μ increases, L_3 moves away from the first primary P_1.

3.3.2 Variations in amplitude of halo orbits

The change in the x-amplitude of halo orbits around L_1 and L_2 corresponding to different values of mass factor are shown in Figs. 3.2. The values of $A_{\tilde{x}}$ are obtained corresponding to $A_{\tilde{z}} = 3.25 \times 10^{-4}$. The value of μ is increased from an initial value 10^{-8} with a fixed step size 10^{-6} until $\mu = 0.5$.

From Fig. 3.2(A), it can be observed that amplitude $A_{\tilde{x}}$ is a monotonically decreasing function of μ while it is a monotonically increasing function of μ for halo orbits around L_2 (3.2(B)). In Tables 3.1 and 3.2, the values of $A_{\tilde{x}}$ corresponding to $A_{\tilde{z}} = 3.25 \times 10^{-4}$ are given. From Table 3.1, it can be verified that the value of $A_{\tilde{x}}$ decreases with the increase in the value of mass factor which indicates that amplitude $A_{\tilde{x}}$ is a decreasing function of mass factor μ. Table. 3.2 shows amplitude of halo orbits around L_2 increases with the increase in the mass factor, so it can be concluded that $A_{\tilde{x}}$ is a increasing function of μ. Table 3.3 shows that amplitude of halo orbits around L_3 increases with the increase in the mass factor. Here, $A_{\tilde{x}} = 0.045$ is taken for getting the corresponding value of $A_{\tilde{z}}$.

3.3.3 Variations in period and size of halo orbits

In Figs. 3.3, variations in period of halo orbits around L_1 and L_2 corresponding to different values of $\mu \in [10^{-8}, 0.5]$ are shown. Due to increase in the value of mass factor, period of orbits around L_1 decreases (Fig. 3.3(A)) while period of orbits around L_2 increases (Fig. 3.3(B)). Fig. 3.3(A) shows period of halo orbits around L_1 and μ are related by a non-linear monotonically decreasing function. Period of halo orbits around L_2 can be expressed as non-linear monotonically increasing function of μ (Fig. 3.3(B)). The data of Tables 3.1 and 3.2 also agree with above conclusions. From Table 3.3, it can be observed that period of halo orbits around L_3 decreases with the increase in

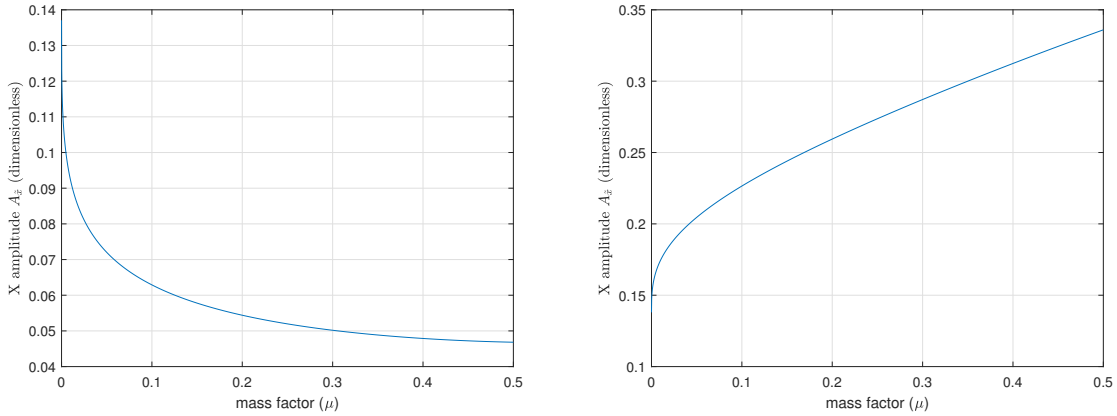

(A) Variation in x-amplitude for halo obits around L_1 against variation in μ

(B) Variation in x-amplitude for halo orbits around L_2 against variation in μ

FIGURE 3.2: Variation in x-amplitude for halo orbits around Lagrangian points against variation in mass factor

mass factor of primaries.

In Fig. 3.4, halo orbits around L_1 and L_2 are plotted in dimensionless system for $\mu \in [10^{-8}, 0.5]$. In this case, starting with $\mu = 10^{-8}$, value of μ is increased by 10^{-2} till $\mu = 0.5$. As μ increases, orbits around L_1 elongate and move closer to the first primary, P_1, as can be seen in Fig. 3.4(A). Orbits around L_2 also elongate as mass factor increases. As the value of μ increases and $\mu \leqslant \mu_0$, halo orbits around L_2 move away from the second primary and for $\mu \geqslant \mu_0$, these orbits come closer to the second primary. Halo orbits in the Sun-Mars, Sun-Earth, Sun-Uranus, Sun-Saturn and Sun-Jupiter system are plotted in Fig. 3.5 in blue, red, cyan, green and magenta colour, respectively.
From Fig. 3.5(A), it can be observed that as mass factor increases, halo orbits shift towards the Sun whereas from Fig. 3.5(B), it can be observed that halo orbits around L_2 move away from the planets due to increase in mass factor. In both the cases, orbits enlarge as mass factor increases.

3.3.4 Variations in initial position and velocity of spacecraft

For different values of μ in the interval $[10^{-8}, 0.5]$, the distance between the origin and the initial position of spacecraft is measured. Also, the initial velocity of the spacecraft is measured for $\mu \in [10^{-8}, 0.5]$.

In Fig. 3.6, the distance between the origin and spacecraft and initial velocity of the spacecraft moving in a halo orbit around L_1 is given. Fig. 3.6(A) shows that

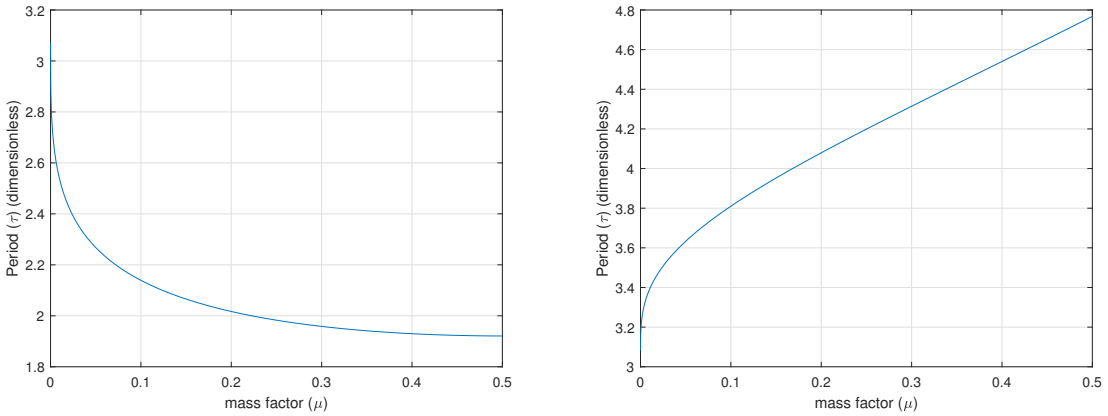

(A) Variation in period of halo orbits about L_1 against μ (B) Variation in period of halo orbits around L_2 against μ

FIGURE 3.3: Variation in period of halo orbits around Lagrangian points against variation in mass ratio

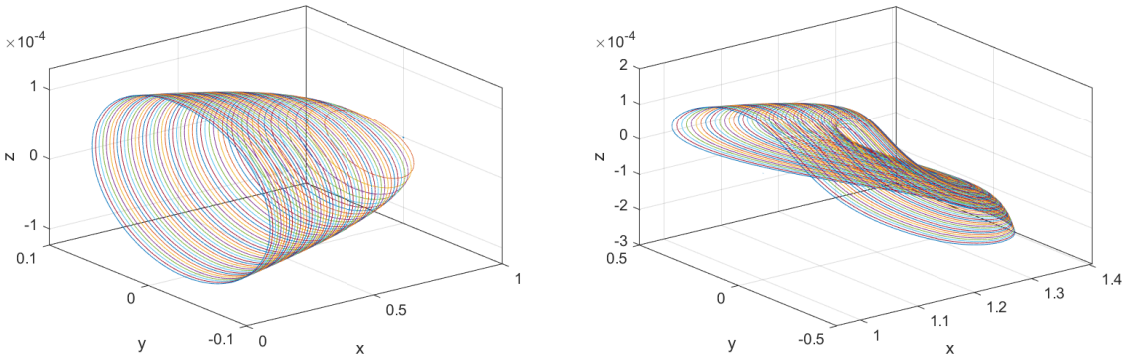

(A) Halo orbits around L_1 (dimensionless) (B) Halo orbits around L_2 (dimensionless)

FIGURE 3.4: Change in size of halo orbits against mass ratio

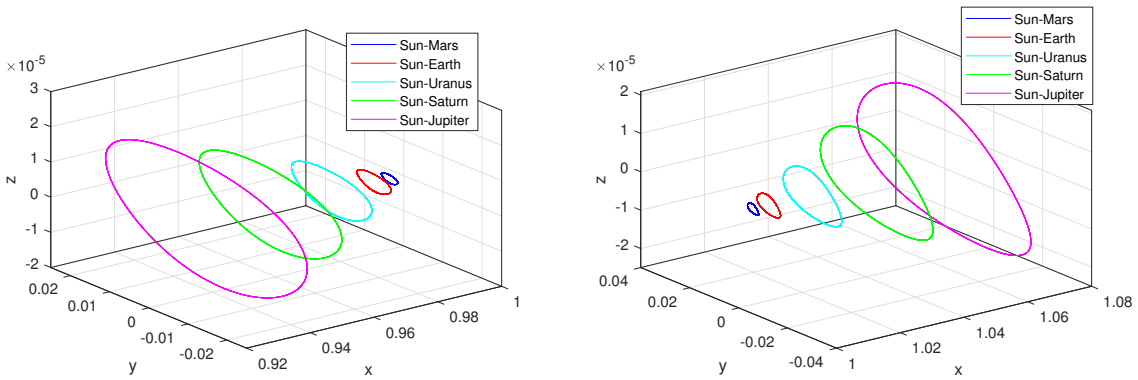

(A) Halo orbits around Sun-Planet L_1 (dimensionless) (B) Halo orbits around Sun-Planet L_2 (dimensionless)

FIGURE 3.5: Halo orbits around L_1 and L_2 for Sun-Planet systems

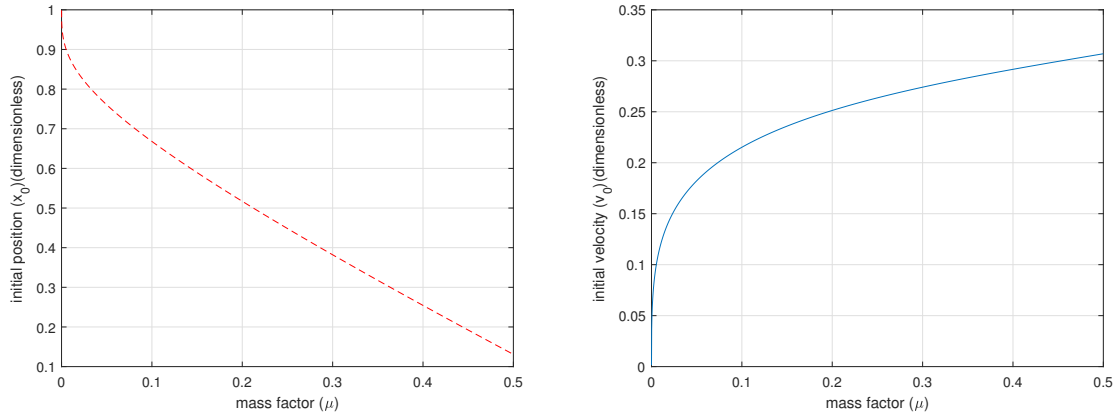

(A) Distance of spacecraft from origin for halo orbits around L_1

(B) Initial velocity of spacecraft for halo orbits around L_1

FIGURE 3.6: Variation in initial distance and velocity of spacecraft for halo orbits around L_1 against variation in mass ratio

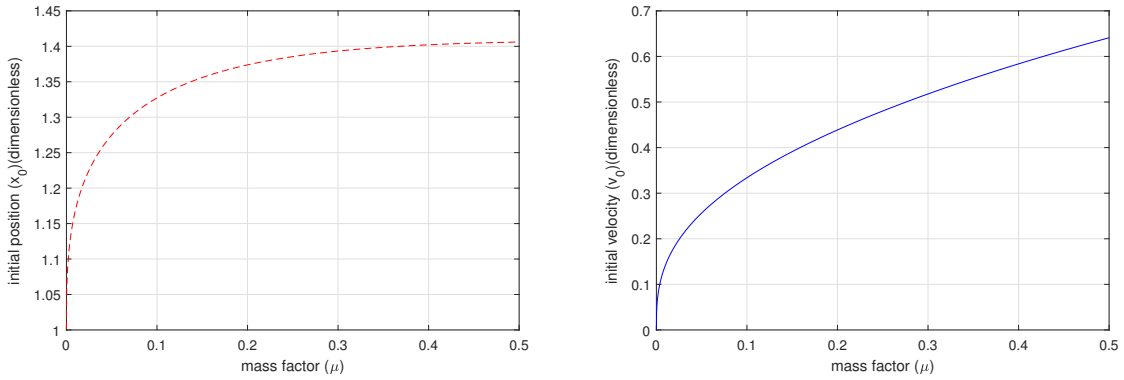

(A) Distance of spacecraft from origin for halo orbits around L_2

(B) Initial velocity of spacecraft for halo orbits around L_2

FIGURE 3.7: Variation in initial distance and velocity of spacecraft for halo orbits around L_2 against variation in mass ratio

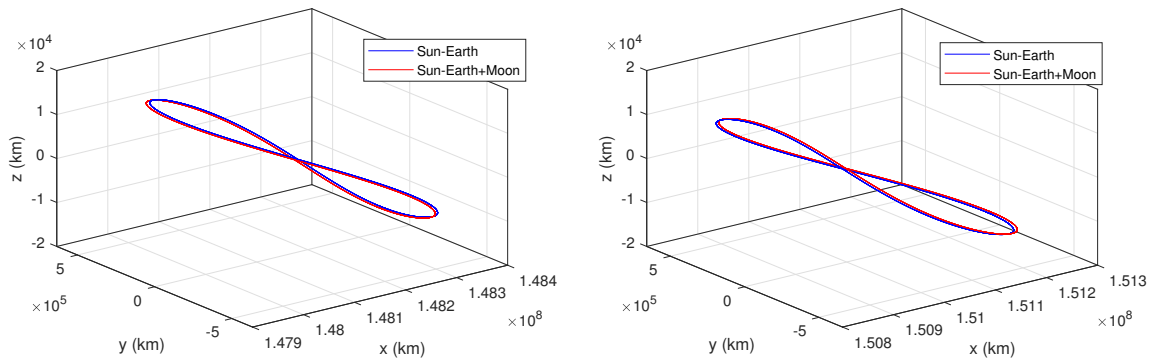

(A) Halo orbits around Sun-Earth+Moon L_1

(B) Halo orbits around Sun-Earth+Moon L_2

FIGURE 3.8: Halo orbits around L_1 and L_2 for Sun-Earth and Sun-Earth+Moon systems

as μ increases, spacecraft goes nearer to the origin and its initial velocity increases (Fig. 3.6(B)). Data of Table 3.1 agrees with these observations. In Fig. 3.7, the distance between the origin and the spacecraft and velocity of the spacecraft at initial time for halo orbits around L_2 are given. From Fig. 3.7(A), it can be observed that as the mass factor of primaries increases, the distance between the spacecraft and the origin increases. Also, Fig. 3.7(B) shows that the initial velocity of spacecraft increases due to increase in the mass factor. From Table 3.2, it can be verified that above results hold true in various Sun-Planet systems as well.

In Fig. 3.8, halo orbits around L_1 and L_2 in the Sun-Earth and Sun-Earth+Moon system are plotted in blue and red colour, respectively. Data of location of Lagrangian points and corresponding parameters of halo orbits in these systems are given in Table 3.4. Here, the distances are in kilometers, period is in days and velocity is in km/s. In the Sun-Earth system, the Sun is the first primary and the Earth is the second primary while in the Sun-Earth + Moon system, the Sun is the first primary and the Earth and the Moon together is considered to be a single massive body which is considered to be the second primary. In this case, the mass of the second primary is the total of the mass of the Earth and the mass of the Moon.

The difference between the mass factors of these two systems is 3.69124×10^{-8}, a small quantity, but remarkable variations in parameters of halo orbits are observed. Lagrangian point L_1 shifts 5991.112 km towards the Sun in the Sun-Earth + Moon system and $A_{\tilde{x}}$ of this system is 3092.673 km less than $A_{\tilde{x}}$ of the Sun-Earth system. Further, the spacecraft comes closer to the origin by 5101.5238 km and initial velocity increases by 5688.5119 km/s in the Sun-Earth + Moon system. Similarly, Lagrangian point L_2 shifts 6140.872 km towards the Earth, $A_{\tilde{x}}$ increases by 2322.344 km, spacecraft goes away from the origin by 6868.3517 km and initial velocity increases by 5421.4063 km/s in the Sun-Earth + Moon system. In both the cases, $A_{\tilde{z}} = 1.5 \times 10^6$ km is taken for getting corresponding $A_{\tilde{x}}$ for halo orbits around both the collinear Lagrangian points.

3.4 Conclusions

In this chapter, effects of mass factor of primaries on parameters of halo orbits around collinear Lagrangian points L_1, L_2 and L_3 in CRTBP are studied. For this analysis, different values of μ in the interval $[10^{-8}, 0.5]$ are considered and the results are verified

by finding halo orbits in the Sun-Mars, Sun-Earth, Sun-Uranus, Sun-Saturn and Sun-Jupiter system. The perturbations due to oblateness and radiation of the primaries are neglected in the present study.

The analysis shows that due to increase in the mass factor of the primaries, the distance between the second primary and L_1 increases, hence Lagrangian point L_1 move towards the more massive primary. The x amplitude of halo orbits around L_1 decreases due to which the distance between these orbits and the origin decreases. Further, period of these orbits decreases and initial velocity increases due to increase in the mass factor. It is also observed that halo orbits around L_1 enlarge as mass factor increases.

It is observed that due to increase in the mass factor, halo orbits around L_2 elongate and amplitude, period, initial distance from the origin and initial velocity increase. The distance between the Lagrangian point L_2 and the second primary increases with the increase in the mass factor when $\mu \leqslant 0.17894$, hence L_2 moves away from both the primaries. For $\mu \geqslant 0.17894$, orbits come closer to the second primary.

Halo orbits around L_3 move away from the first primary, their amplitude decreases while period increases as the mass factor increases.

Halo orbits around L_1 and L_2 of the Sun-Earth and Sun-Earth + Moon systems are computed in dimensional system. The mass factor of the Sun-Earth + Moon system is 3.69124×10^{-8} more than the mass factor of the Sun-Earth system. Present study shows that even a small increment of order 10^{-8} in the value of mass factor vary the parameters of halo orbits by thousands of kilometers.

It can be concluded that the position of Lagrangian points and the parameters of halo orbits around collinear Lagrangian points are strongly influenced by the mass factor of the primaries.

TABLE 3.4: Parameters of halo orbits about L_1 and L_2 for Sun-Earth and Sun-Earth+Moon systems

	System	mass factor (μ)	Lagrangian point $\times 10^8(km)$	$A_{\bar{x}}$ $\times 10^7(km)$	Period (days)	initial distance $\times 10^8(km)$	initial velocity $\times 10^6(km/s)$
L_1	Sun - Earth	3.0035×10^{-6}	1.48113	1.98232	176.50631	1.48340	1.41198
	Sun - Earth+Moon	3.0404×10^{-6}	1.48107	1.98201	176.49612	1.48334	1.41767
L_2	Sun - Earth	3.0035×10^{-6}	1.51097	2.11632	180.26278	1.51272	1.32090
	Sun - Earth+Moon	3.0404×10^{-6}	1.51103	2.11655	180.26776	1.51278	1.32632